Article

A Real-Time System Status Evaluation Method for Passive UHF RFID Robots in Dynamic Scenarios

Honggang Wang *, Weibing Du *, Bo Qin, Ruoyu Pan and Shengli Pang

School of Communications and Information Engineering, Xi'an University of Posts and Telecommunications, Xi'an 710121, China; qinbo@stu.xupt.edu.cn (B.Q.); panruoyu@xupt.edu.cn (R.P.); pangshengli@xupt.edu.cn (S.P.)
* Correspondence: wanghonggang@xupt.edu.cn (H.W.); duweibing@stu.xupt.edu.cn (W.D.)

Abstract: In dynamic scenarios, the status of a Radio Frequency Identification (RFID) system fluctuates with environmental changes. The key to improving system efficiency lies in the real-time monitoring and evaluation of the system status, along with adaptive adjustments to the system parameters and read algorithms. This paper focuses on the status changes in RFID systems in dynamic scenarios, aiming to enhance system robustness and reading performance, ensuring high link quality, reasonable resource scheduling, and real-time status evaluation under varying conditions. This paper comprehensively considers the system parameter settings in dynamic scenarios, integrating the interaction model between readers and tags. The system's real-time status is evaluated from both the physical layer and the Medium Access Control (MAC) layer perspectives. For the physical layer, a link quality evaluation model based on Uniform Manifold Approximation and Projection (UMAP) and K-Means clustering is proposed from the link quality. For the MAC layer, a multi-criteria decision-making evaluation model based on combined weighting and the Technique for Order Preference by Similarity to Ideal Solution (TOPSIS) is proposed, which comprehensively considers both subjective and objective factors, utilizing the TOPSIS algorithm for an accurate evaluation of the MAC layer system status. For the RFID system, this paper proposes a real-time status evaluation model based on the Classification and Regression Tree (CART), which synthesizes the evaluation results of the physical layer and MAC layer. Finally, engineering tests and verification were conducted on the RFID robot system in mobile scenarios. The results showed that the clustering average silhouette coefficient of the physical layer link quality evaluation model based on K-Means was 0.70184, indicating a relatively good clustering effect. The system status evaluation model of the MAC layer, based on the combined weighting-TOPSIS method, demonstrated good flexibility and generalization. The real-time status evaluation model of the RFID system, based on CART, achieved a classification accuracy of 98.3%, with an algorithm runtime of 0.003 s. Compared with other algorithms, it had a higher classification accuracy and shorter runtime, making it well suited for the real-time evaluation of the RFID robot system's status in dynamic scenarios.

Keywords: dynamic scenarios; RFID robot; system status; combined weighting-TOPSIS; k-means; CART

1. Introduction

UHF passive RFID technology is widely used in the fields of logistics and warehousing [1], anti-counterfeiting and traceability, and apparel retailing [2] due to its advantages of low-cost, long-range, and batch fast identification, and it has had a far-reaching impact on life. However, traditional RFID systems typically employ static deployment and fixed parameter configurations, making it difficult to meet the growing performance demands in complex, large-scale application scenarios, like unmanned warehousing, apparel retail, and library and archive management. In recent years, with the development of RFID technology and the continuous upgrading of industry applications, RFID usage has expanded from static scenarios to dynamic applications, such as mobile robots, drones, and

conveyor belts [3–5]. In these dynamic applications, how to achieve intelligent mobile sensing capabilities for readers has become a key innovation in RFID technology. This not only depends on the integration of RFID systems with technologies like 5G, intelligent computing, automatic control, and deep learning but also reflects the inevitable trend of RFID systems expanding into dynamic application scenarios.

In an RFID system, the tag and the reader are two key components, each with distinct functions within the system. Tags are typically passive elements attached to objects, relying on the energy received from the reader to respond. Passive RFID tags do not require an internal battery and depend on the radio frequency signals emitted by the reader for power. The reader is responsible for emitting electromagnetic waves and receiving reflected signals from the tags to read the tag information. It plays an active role in the RFID system, not only communicating with the tags but also adjusting communication parameters such as power and frequency as needed. The efficiency and performance of the reader directly affect the system's recognition rate, the accuracy of data transmission, and the overall reliability. In dynamic applications, the mobility of the reader and its real-time status evaluation mechanism are crucial factors influencing the stability of the system.

The integration of mobile robots and RFID technology has become an important approach for achieving mobile recognition through readers. In the integration of RFID technology with mobile robots, several innovative applications have already emerged, for instance, LibBot [6], which is used for automated inventory and location detection of books; MONITOR [7], which is equipped with a rotating antenna and uses synthetic aperture radar (SAR) for high-precision 3D positioning; CultureID [8], which can create a 3D map of its surrounding environment and autonomously navigate and locate within the map; and an obstacle avoidance robot [9] that builds an obstacle avoidance system by using automatically tuned RFID tags on obstacles as near-field coupling detectors. These applications demonstrate the vast potential for the integration of RFID and robotics technology.

In dynamic scenarios, the relative position between readers and tags, the number of tags, and the identification medium are constantly changing. These factors directly affect the efficiency and stability of the RFID system. Therefore, ensuring the efficient operation of the system in dynamic scenarios depends on the real-time evaluation of the system's status and the corresponding dynamic adjustments to the parameters. Compared to traditional static RFID deployment scenarios or applications involving tag movement [10,11], dynamic scenarios where the reader is moving are more complex, posing greater demands on the evaluation of the RFID system's status. However, there is relatively little research on the performance of RFID systems under the movement of readers in dynamic scenarios, which also presents new challenges for system optimization.

In static scenarios, some scholars have already conducted research on the state of RFID systems. For instance, K. M. Ramakrishnan [12] and ODIN [13] each carried out basic evaluations of system state metrics and established foundational assessment benchmarks. S. R. Aroor [14] studied the read range and recognition speed of tags in different medium environments, while M. Periyasamy [15] delved into the changes in the read range and read count of tags when placed near various media. Tianbao Li [16] introduced the concept of a "set of metrics" and explored read speed, read range, and power attenuation in depth. However, compared to static scenarios, the identification environment in dynamic scenarios is more complex. The interaction environment between the reader and the tags changes rapidly, with factors such as the identification environment, tag quantity, and medium characteristics of the RFID system constantly in flux. For example, in mobile robotics applications, as the reader moves, the system's physical environment may experience issues like reflection, interference, and occlusion, leading to unstable link quality. Simultaneously, the relative motion between the reader and the tags requires the communication MAC layer protocol to dynamically adapt to these changes. If key parameters of the RFID system are not promptly adjusted according to changes in the system state, it can result in decreased identification accuracy and efficiency, thereby affecting system reliability. Therefore, establishing a real-time system state evaluation mechanism is not only central

to ensuring the performance of dynamic RFID systems but also key to their ability to meet future challenges in complex application scenarios and evolve toward a high level of intelligence.

This paper primarily addresses the dynamic issue of reader movement and fixed tags. It first explains the importance of real-time status evaluation of RFID systems in dynamic scenarios and deeply analyzes the system's status from both the physical layer and MAC layer perspectives. It then constructs a physical layer link quality evaluation model and a MAC layer system status evaluation model. Next, a real-time status evaluation method suitable for dynamic scenarios in UHF passive RFID robot systems is proposed. Finally, the aforementioned models are validated to ensure their effectiveness and reliability.

The remaining sections of this paper are arranged as follows: Section 2 introduces the RFID system status in dynamic scenarios; Section 3 proposes a real-time evaluation model and theoretical algorithms for the system status at the physical layer; Section 4 proposes a real-time evaluation model and theoretical algorithms for the system status at the MAC layer; Section 5 combines the evaluation results of the physical and MAC layers to propose a real-time evaluation model and theoretical algorithms for the RFID system status; Section 6 conducts tests in dynamic scenarios and performs the calculation and analysis of real-time status evaluations for the RFID robot system; and Section 7 concludes this paper.

2. Dynamic Scenario RFID System Status

2.1. RFID Dynamic Identification Scenarios

A typical application of RFID is usually static identification, where tags are identified through fixed checkpoints, channels, or handheld devices. In a static RFID system, the air interface parameter Q dynamically adjusts the frame length based on the collision situation of the tags within the reader's identification range, thereby improving the system's channel utilization.

In dynamic scenarios, RFID applications are no longer limited to fixed locations; tags can be placed on conveyor belts and assembly lines or readers can be installed in mobile robots, drones, AGVs (Automated Guided Vehicles), and other mobile equipment to achieve mobile identification. With the development of technology and increased industrial demand, RFID dynamic identification will gradually replace static identification to achieve mobile identification and intelligent inventory.

In dynamic identification scenarios, the reader and tag are always in relative motion, and the problem of random post-identification and missed reads of the tag can lead to reduced efficiency of the RFID system. The complexity of dynamic identification scenarios limits the ability of traditional Q-algorithms in improving performance and system efficiency. In this paper, we take the RFID robot system as an example and use machine learning methods to perform operations, such as real-time evaluation, clustering, and prediction of the system status and physical link, to realize the intelligent perception of the RFID system status and adaptive adjustment of the system parameters.

2.2. Real-Time Status Evaluation of RFID Systems

In RFID technology, the stability of the system status is critical to ensure efficient identification. In static RFID systems, readers and tags are in a fixed position and use preset parameters, and factors such as the reader recognition environment, number of tags, and media remain unchanged, so the system status is relatively stable. However, in dynamic scenarios, readers and tags are always in relative motion; the reader identification environment, number of tags, tag space layout, link status, and other elements of real-time changes result in the RFID system status being continually affected by dynamic factors, showing dynamic changes in the characteristics.

As shown in Figure 1, this paper provides a comprehensive assessment of the RFID system status from both the physical and MAC layer perspectives. The physical layer analysis focuses on the fluctuation of the channel interference and link quality, which are significantly reflected in the statistical characteristics of an RSSI (Received Signal

Strength Indicator). The MAC layer analysis mainly focuses on the impact of the real-time adjustment of air interface parameters on the system status, which are reflected in the key performance indicators, such as time efficiency, identification efficiency, and throughput. Through this multi-dimensional analysis, this paper aims to provide a theoretical basis for the status evaluation and parameter optimization of RFID systems.
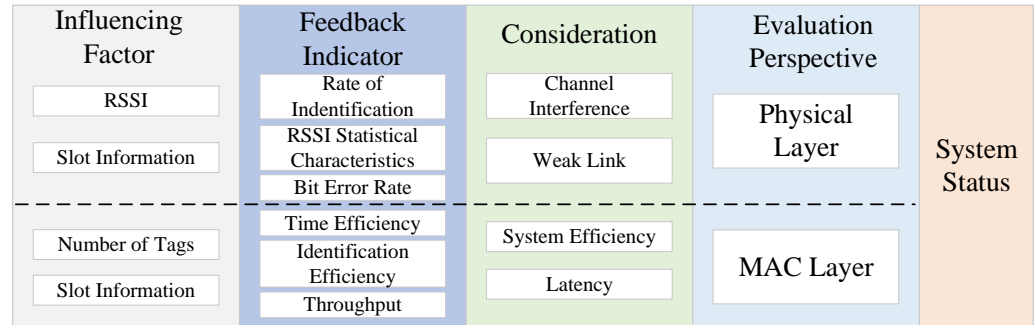
Influencing Factor	Feedback Indicator	Consideration	Evaluation Perspective	System Status
RSSI	Rate of Indentification	Channel Interference	Physical Layer	
Slot Information	RSSI Statistical Characteristics	Weak Link		
	Bit Error Rate			
Number of Tags	Time Efficiency	System Efficiency	MAC Layer	
Slot Information	Identification Efficiency	Latency		
	Throughput			

Figure 1. System status evaluation plan.

3. Physical Layer System Status Evaluation

The physical layer in an RFID system is the basis for data transmission and is responsible for signal modulation and demodulation, transmission rate control, and ensuring the integrity and reliability of data transmission. Therefore, the quality of the communication link is crucial to the normal operation of the physical layer. A high-quality link not only improves the data transmission efficiency but also ensures the accuracy and reliability of the data, indirectly affecting the overall performance of the RFID system.

To ensure the optimal performance of the physical layer, this paper proposes a real-time evaluation method based on link quality. By monitoring and analyzing the link quality, the physical layer system status changes are captured in time, providing an accurate basis for system optimization and adjustment. The evaluation not only reflects the current link status but also predicts potential communication problems to guarantee the stable operation of the RFID system.

3.1. Performance Indicators

Link quality is an important metric used to describe the reliability and stability of signal transmission in communication systems, and it can be evaluated from multiple perspectives. Depending on the method of acquisition, link quality can be classified into hard metrics and soft metrics. Based on the characteristics of the RFID system, this paper evaluates link quality through the rate of identification, the number of inventory cycles, the bit error rate, and the RSSI.

3.1.1. Rate of Identification

In dynamic scenarios, RFID systems can be piggybacked on mobile robots for identification. As the robot moves, the identification range of the reader is constantly moving. As shown in Figure 2, the archive shelf evenly distributes a number of RFID tags that are attached to the file. The reader at speed v is in front of the archive shelf mobile scanning, with the movement of the reader constantly having the old tag leaving the identification area and the new tag moving into the identification area.
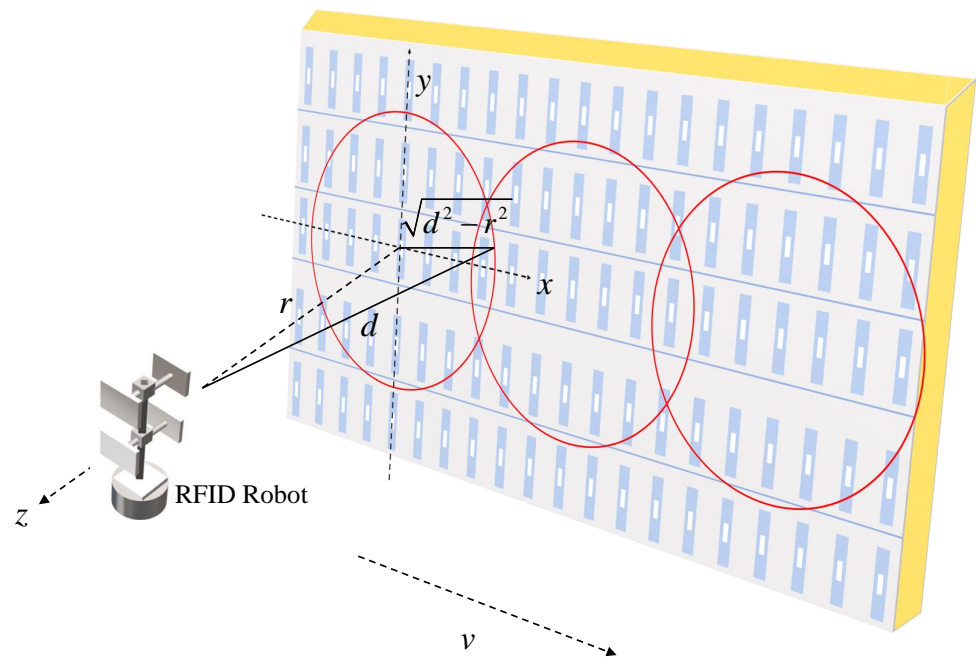
Figure 2. Reader identification process, where the red circle indicates the identification range of the reader.

The relationship between the reader transmit power and signal propagation distance in UHF passive RFID systems can be derived from the Friis equation:

$$P_r = \frac{P_t G_r G_t \lambda^2 K}{(4\pi d)^2} \tag{1}$$

$$d \leq \frac{\lambda^2}{4\pi} \sqrt{\frac{P_t G_r G_t \tau}{P_{th}} \eta} \tag{2}$$

where P_r is the tag backscattered power received by the reader; P_t is the transmitter power of the reader; P_{th} is the tag activation sensitivity; G_r and G_t are the antenna gain of the reader and tag, respectively; λ is the signal wavelength; d is the distance from the reader to the tag; K is the antenna loading impedance matching coefficient; τ is the tag power transfer coefficient; and η is the conversion efficiency, and in the practical environment, it is generally taken as $\tau = 0.25$ and $\eta = 0.25$.

According to Equation (2), the distance between the reader and the farthest tag within the identification range is denoted as d. The identification range varies depending on the horizontal distance r between the reader and the tag during the identification process, as shown in Figure 2. Based on the calculations, the diameter of the identification range is $2\sqrt{d^2 - r^2}$, and the area of the identification range is $S = \pi(d^2 - r^2)$.

The effective scanning area of the reader can be categorized into primary and secondary detection regions. In the primary detection region, the probability that most tags can be detected is close to 100%, while in the secondary detection region, the probability that tags are detected is negligible [17]. Therefore, in this paper, the reader identification range is specified as the rectangular region formed by the two dashed lines in Figure 3, i.e., the primary detection region, ignoring the identification of tags on both sides.

There are m_{total} tags evenly distributed on a shelf with a length of l and c layers, and each layer has a height of h. The number of tags per unit length on each layer is $\frac{m_{total}}{cl}$. A robot moves at a constant speed of v m/s, and the reading range diameter of the reader is $2\sqrt{d^2 - r^2}$.
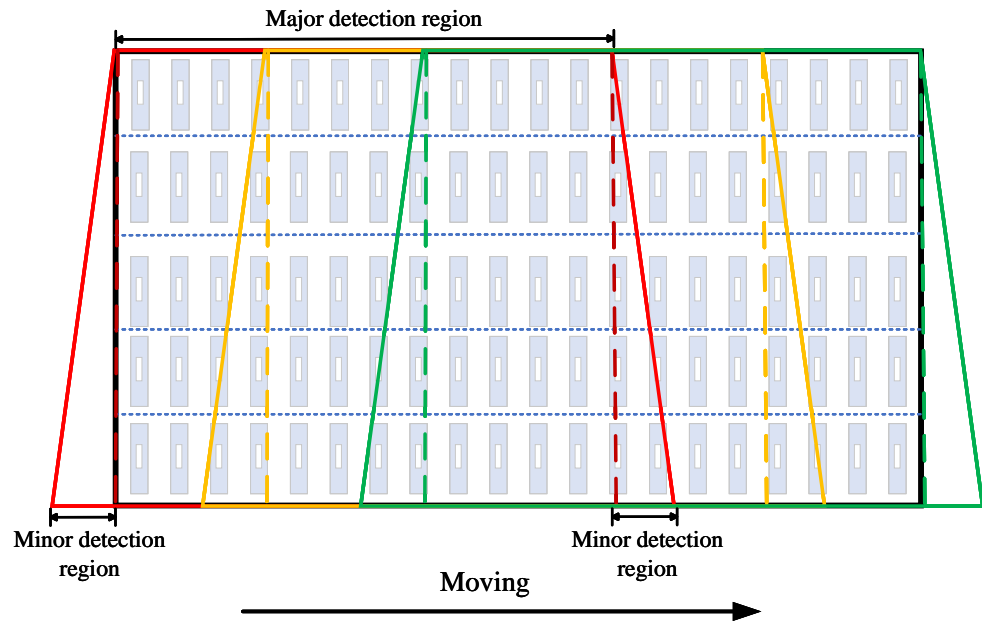
Figure 3. Reader identification range optimization, where different colors indicate different identification ranges.

When $\dfrac{2\sqrt{d^2-r^2}}{h} < c$, if c is odd, the number of layers of the shelf within the reading range of the antenna is $a = \text{round}\left(\dfrac{2\sqrt{d^2-r^2}}{h}\right)$, and if c is even, the number of layers of the shelf within the reading range of the antenna is $a = \left\lfloor \dfrac{2\sqrt{d^2-r^2}}{h} \right\rfloor$. The number of tags entering the reader's detection range per unit time is $n = a \cdot \dfrac{m_{total}}{cl} \cdot v$.

When $\dfrac{2\sqrt{d^2-r^2}}{h} \geq c$, the number of tags entering the reader's detection range per unit time is $n = \dfrac{m_{total}}{l} \cdot v$, which represents the number of newly detected tags in theory. Therefore, the number of tags successfully identified by the reader at second t is as follows:

$$m_t = n \cdot t \tag{3}$$

The actual number of tags successfully identified by the RFID system is $m_{success}$ and then the rate of identification for the system at second t is as follows:

$$RoI = \frac{m_{success}}{m_t} = \frac{m_{success}}{n \cdot t} \tag{4}$$

3.1.2. RSSI

In RFID systems, the RSSI is sensitive to environmental changes and easy to obtain. A high RSSI usually indicates good communication quality, so using the RSSI as a performance metric helps accurately evaluate the link quality.

In dynamic scenarios, factors such as reader identification of the scenario, varying distances between the reader and tags, and other continuously changing conditions affect the RSSI. Therefore, this study comprehensively considers both the average level and the degree of volatility of the RSSI to evaluate the impact of environmental factors.

(1) Average level of RSSI

Define $\overline{RSSI}$ as the average RSSI within a unit of time, reflecting the overall level of the RSSI during that time.

$$\overline{RSSI} = \frac{1}{n} \sum_{i=1}^{n} RSSI_i \tag{5}$$

where $RSSI_i$ denotes the RSSI at time i and n denotes the number of RSSI samples per unit time.

(2) Degree of volatility of RSSI

Define σ^2_{RSSI} as the variance of the RSSI per unit time, reflecting the stability of the RSSI per unit time.

$$\sigma^2_{RSSI} = \frac{1}{n} \sum_{i=1}^{n} \left(\overline{RSSI} - RSSI_i \right)^2 \tag{6}$$

Define Skewness and Kurtosis as the standard third-order central moment and standard fourth-order central moment of the RSSI per unit time, describing the asymmetry and steepness of the distribution of the RSSI per unit time, which facilitates the identification of anomalies, such as sudden signal attenuation or enhancement reflecting rapid changes in the environment.

A skewness value of zero indicates a symmetric data distribution; a positive value indicates that the tail extends to the right and there are periods of extremely good link quality; and a negative value indicates that the tail extends to the left and there are periods of extremely poor link quality.

High kurtosis means that extreme values lead to increased variance and is often used to characterize the link quality distribution. High kurtosis indicates that the data have sharp peaks and thick tails, and the link quality fluctuates between extremely good or extremely poor; low kurtosis indicates that the data distribution is flat and the link quality is more stable.

$$Skewness = \frac{n}{(n-1)(n-2)} \sum_{i=1}^{n} \left[\frac{RSSI_i - \overline{RSSI}}{\sigma_{RSSI}} \right]^3 \tag{7}$$

$$Kurtosis = \frac{n(n+1)}{(n-1)(n-2)(n-3)} \sum_{i=1}^{n} \left[\frac{RSSI_i - \overline{RSSI}}{\sigma_{RSSI}} \right]^4 - \frac{3(n-1)^2}{(n-2)(n-3)} - 3 \tag{8}$$

Define the Link Quality Volatility Indicator (LQVI) with the following equation:

$$LQVI = w_1 \cdot \sigma^2_{RSSI} + w_2 \cdot Skewness + w_3 \cdot Kurtosis \tag{9}$$

where w_1, w_2, and w_3 are the indicator weights of the σ^2_{RSSI}, *Skewness*, and *Kurtosis* determined using the entropy weighting method.

3.1.3. Bit Error Rate

The bit error rate (BER) is an important measure of link quality, reflecting the proportion of erroneous bits in data transmission. In RFID systems, due to the nature of wireless communication, evaluating the BER is critical to ensure data accuracy and system reliability. However, the BER in RFID systems is usually difficult to measure directly, so this paper determines the generation of the BER by analyzing the interaction process between the reader and the tag.

BERs in RFID systems typically occur at two stages. The first is when the tag sends an RN16 to the reader, and although the reader is able to detect a completely tampered RN16, individual bit errors cannot be detected, which results in the reader sending an ACK with an invalid RN16 that cannot be answered by the tag. Secondly, when the tag transmits its ID number in response to the reader's ACK command, the error will be detected by the CRC (Cyclic Redundancy Check).

Based on the analysis of the interaction commands between the reader and the tag in Section 4.1, this paper considers the reader's successful reading to occur when it sends a QueryRepeat command after sending the ACK command; otherwise, the time slot is regarded as an error slot.

The BER is defined as the ratio of the number of bit error slots to the total number of slots within a unit of time.

$$BER = \frac{n_{error}}{n} \tag{10}$$

where n is the total number of slots within a unit time, and n_{error} is the number of slots in which bit errors occur within a unit time.

3.2. A Physical Layer System Status Evaluation Model Based on UMAP and K-Means

In wireless sensor networks (WSNs), traditional link quality evaluation is typically based on dividing the link into different levels according to its packet reception rate (PRR). Data with the same link quality level exhibit certain similarities, while data samples of different levels demonstrate distinct patterns. Based on the regularity of data similarity, this paper adopts the UMAP and K-Means algorithms to evaluate link quality through the performance metrics discussed in Section 3.1.

This section's evaluation model construction is divided into two parts: UMAP-based link feature extraction and a K-Means-based link quality evaluation model.

3.2.1. Link Feature Extraction Based on UMAP

UMAP (Uniform Manifold Approximation and Projection) is a nonlinear technique used for dimensionality reduction and visualization. It works by constructing a graph of neighboring points in high-dimensional space and optimizing the low-dimensional embedding while preserving both local and global structures of the data [18]. UMAP is computationally efficient, scalable, and flexible in terms of parameters, making it widely used in the field of machine learning. Its algorithmic process is as follows:

Step 1: Data preprocessing. Standardize the original data so that each feature has a mean of 0 and a variance of 1, eliminating the scale differences between different features.

Step 2: Build high-dimensional neighborhood graph. Use the KNN (k-nearest neighbors) algorithm to find the k-nearest neighbors for each data point. Utilize a Gaussian kernel function to calculate the edge weights in the high-dimensional neighborhood graph, representing the similarity between the data. The weight calculation is as follows:

$$w_{ij} = \exp\left(-\frac{d_{ij}^2 - \rho_i}{\sigma_i}\right) \tag{11}$$

where d_{ij} is the distance between data i and j, ρ_i is the distance threshold used to control the local density, and σ_i is the local scale parameter.

Step 3: Initialize the low-dimensional embedding. Use random initialization or other dimensionality reduction algorithms to generate the initial points of the low-dimensional embedding. The weights in the low dimensional space are calculated as follows:

$$w_{ij}' = \frac{1}{1 + a \cdot (d_{ij}')^{2b}} \tag{12}$$

where d_{ij}' denotes the distance between data points i and j in the low-dimensional space, and a is a hyperparameter to adjust the distance distribution in the low-dimensional space.

Step 4: Optimize the low-dimensional embedding. Use gradient descent to compute the gradient of the objective function, and update the positions of the low-dimensional embeddings based on the gradient. The objective function typically used is cross-entropy, which measures the difference in neighborhood similarity between the high-dimensional and low-dimensional spaces. The function is as follows:

$$C = \sum_{(i,j)} w_{ij} \log\left(\frac{w_{ij}}{w_{ij}'}\right) + (1 - w_{ij}) \log\left(\frac{1 - w_{ij}}{1 - w_{ij}'}\right) \tag{13}$$

Step 5: Repeat the above steps until the objective function converges or the predefined number of iterations is reached.

3.2.2. Link Quality Evaluation Based on K-Means

K-Means is a commonly used clustering algorithm that divides data points into K clusters, maximizing the similarity of data points within the same cluster while minimizing the similarity between data points in different clusters [19]. The K-Means algorithm has low time complexity, making it suitable for handling large datasets, and its implementation and results are easy to interpret. The clustering method is shown in Algorithm 1.

Algorithm 1 K-Means clustering algorithm

1: **Input**: sample set $X = \{x_1, x_2, \cdots, x_m\}$, number of clusters k
2: **Output**: Cluster partition $C = \{C_1, C_2, \cdots, C_k\}$
3: Randomly select k samples from X as the initial cluster centers $\{\mu_1, \mu_2, \cdots, \mu_k\}$
4: **repeat**
5:     **for** $i = 1, 2, \cdots, k$ **do**
6:         Let $C_i = \varnothing \, (1 \leq i \leq k)$
7:     **end for**
8:     **for** $j = 1, 2, \cdots, m$ **do**
9:         Calculate the distance between sample x_j and each cluster center μ_i: $d_{ij} = \|x_j - \mu_i\|_2$
10:         Determine the cluster label of x_j based on the nearest cluster center: $\lambda_j = \arg\min_{i \in \{1,2,\ldots,k\}} d_{ij}$
11:         Assign sample x_j to the corresponding cluster: $C_{\lambda_j} = C_{\lambda_j} \cup \{x_j\}$
12:     **end for**
13:     **for** $i = 1, 2, \cdots, k$ **do**
14:         Calculate new cluster centers: $\mu_i' = \frac{1}{|C_i|} \sum_{x \in C_i} x$
15:     **end for**
16:     **for** $i = 1, 2, \cdots, k$ **do**
17:         **if** $\mu_i' \neq \mu_i$ **then**
18:             Update the current cluster center μ_i to μ_i'
19:         **else**
20:             Keep the current cluster centers unchanged
21:         **end if**
22:     **end for**
23: **until** The current cluster centers have not been updated

---

Furthermore, based on the clustering results, record the upper and lower limits of each parameter in each cluster, determine the parameter range for each level, and establish the relationship between the link level and score as shown in Table 1.

Table 1. Relationship between link level and score.

Link Level	Level Scoring (%)
Class I	100∼81
Class II	80∼61
Class III	60∼41
Class IV	40∼21
Class V	20∼1

The silhouette coefficient is an important metric for evaluating the quality of clustering [20]. It reflects the effectiveness of clustering by evaluating how well a sample is positioned within its assigned cluster. The silhouette coefficient has a range of $[-1, 1]$,

where a higher value indicates that the sample is better positioned within its cluster and the clustering performance is better. The calculation formula is as follows:

$$S_i = \frac{b_i - a_i}{\max(a_i, b_i)} \tag{14}$$

where a_i is the average distance between the i-th sample and all the other samples in the same cluster, and b_i is the average distance between the i-th sample and all the samples in its nearest neighbor cluster.

In this paper, the mean silhouette coefficient (MSC) is used to evaluate the overall clustering performance. The higher the MSC value, the better the clustering result. The calculation formula is as follows:

$$MSC = \frac{1}{n} \sum_{i=1}^{n} S_i \tag{15}$$

where n is the total number of samples, and S_i is the silhouette coefficient of the i-th sample.

Further, based on the clustering results, determine the link level of the samples and calculate the proximity of the sample parameters to the upper and lower limits of the link level parameters, thereby accurately mapping the link level score.

The calculation formula for the closeness degree d_i of the i-th index is as follows:

$$d_i = \frac{\min(|x_i - l_{ij}^1|, |x_i - l_{ij}^2|)}{|l_{ij}^2 - l_{ij}^1|} \tag{16}$$

where x_i is the i-th metric of the link, and l_{ij}^1 and l_{ij}^2 are the lower and upper limits of the metric's range at the j-th level, respectively.

The composite closeness C is as follows:

$$C = \frac{1}{n} \sum_{i=1}^{n} \frac{1}{1 + d_i^2} \tag{17}$$

where n is the total number of indicators.

Then, the group of parameters corresponds to the score:

$$score = \frac{C - C_{\min}}{C_{\max} - C_{\min}} \times (S_{\max} - S_{\min}) + S_{\min} \tag{18}$$

where $C_{\min}$ is the minimum value of the composite closeness, which is usually 0; $C_{\max}$ is the maximum value of the composite closeness, which is usually 1; and $[S_{\min}, S_{\max}]$ is the range of the current grade rating.

4. MAC Layer System Status Evaluation

In an RFID system, the MAC layer plays a critical role in the system's efficient operation and stability and is closely related to the implementation of the tag anti-collision protocol. It is responsible for coordinating communication between multiple tags and the reader, ensuring orderly and efficient data transmission.

Existing tag anti-collision protocols are typically based on a core assumption: no new tags will enter the reader's identification area during the identification process. This assumption allows the protocol to accurately estimate the number of tags to be identified in the current stage based on the identification situation in the previous stage, thereby setting optimal operating parameters. However, in dynamic scenarios, this assumption no longer holds. The dynamic entry and exit of tags during the identification process renders existing protocols unable to adapt to environmental changes, leading to decreased identification performance and even severe tag miss-read issues.

To address the above problems, this paper will focus on studying the performance of readers in mobile multi-tag identification scenarios. By conducting an in-depth analysis of the interaction process between the reader and tags, this paper establishes MAC layer performance indicators based on three aspects, system communication capability, identification capability, and communication efficiency, in order to thoroughly evaluate the system state at the MAC layer.

4.1. Reader–Tag Interaction

The existing RFID anti-collision algorithms are primarily based on improvements to the ALOHA algorithm and the binary tree algorithm. Among them, the EPC C1G2 protocol employs an anti-collision algorithm based on Dynamic Frame-Slotted ALOHA (DFSA) [21]. This algorithm divides the reader's identification process into several frames, with each frame consisting of a number of slots. The number of slots in each frame (i.e., the frame length) is determined by the reader, and the number of slots per frame can vary.

Figure 4 is a link sequence diagram that illustrates the interaction between the reader and the tag. The reader and the tag communicate within the frame slots using commands, such as Query, QueryAdjust, QueryRepeat, and ACK. Depending on the number of tags interacting with the reader within a slot, the frame slots can be classified into three types, idle slot (no tag responds within the slot), successful slot (one tag responds within the slot), and collision slot (multiple tags respond within the slot), as shown in Figure 5.
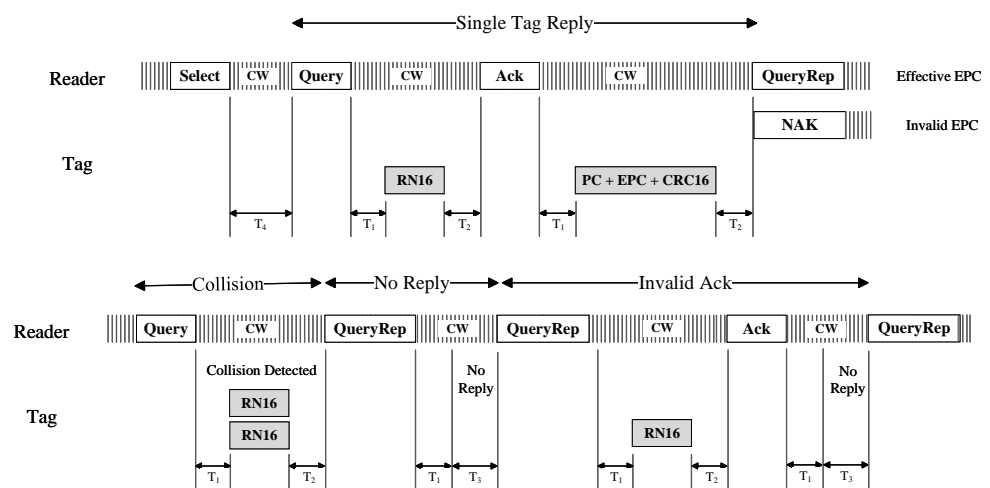

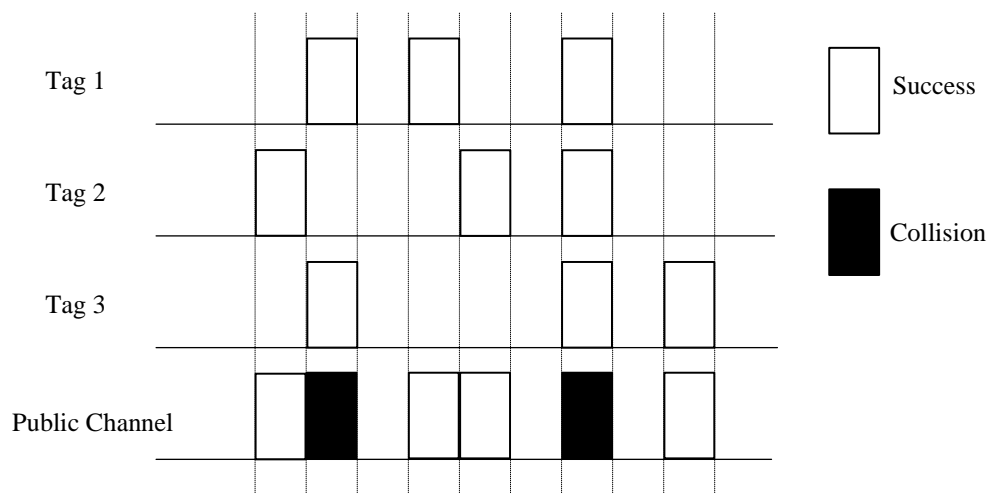**Figure 4.** Link sequence diagram.

Figure 5. Slotted ALOHA algorithm model diagram.

The interaction process between the reader and the tag captured using a spectrum analyzer is shown in Figure 6.
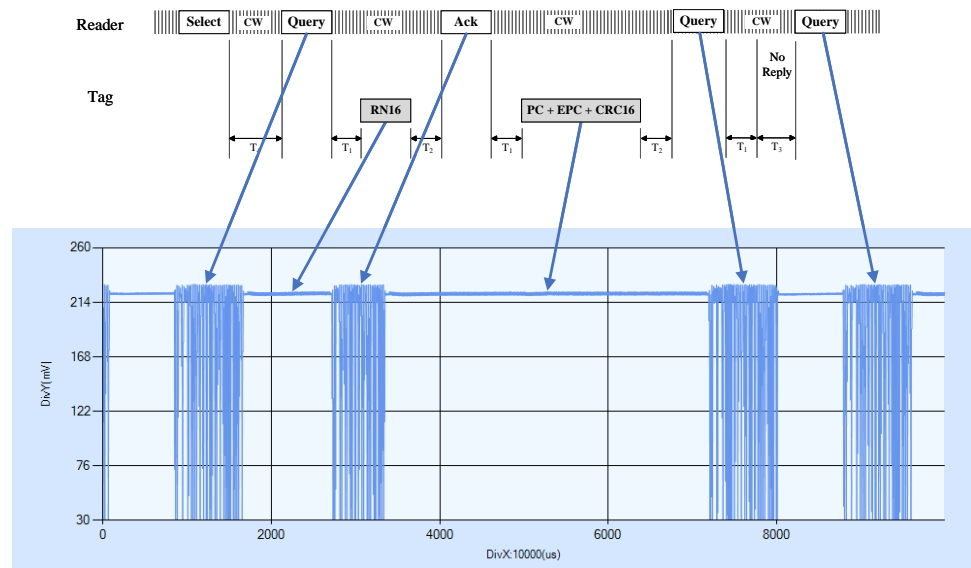

Figure 6. Reader commands and tag responses.

4.2. Construction of MAC Layer Performance Metrics

As shown in Figure 2, the reader identification process is described. For ease of understanding, let us assume the reader is fixed, and the tag enters the reader's identification area from the opposite direction at a speed of v. The reader's identification area has a length of d, and the entire identification area is composed of g consecutive identification frames F_i (where $1 \leq i < g$, and g is the total number of frames during the identification process). Each frame F_i consists of L_i slots, i.e., $F_i = \{f_{ij} \mid j = 1, \ldots, L_i\}$, where L_i is the frame length, and $L_i = E_i + S_i + C_i$, where E_i, S_i, and C_i represent the expected values of idle slots, successful slots, and collision slots, respectively, in frame F_i.

When there are n tags in frame F_i, the probability that k tags fall in the same slot follows a binomial distribution, namely,

$$P(k) = C_n^k \left(\frac{1}{L_i} \right)^k \left(1 - \frac{1}{L_i} \right)^{n-k} \tag{19}$$

The probabilities of successful slots, idle slots, and collision slots are denoted as P_s, P_e, and P_c, respectively:

$$P_s = P(1) = C_n^1 \left(\frac{1}{L_i} \right)^1 \left(1 - \frac{1}{L_i} \right)^{n-1} = \frac{n}{L_i} \left(1 - \frac{1}{L_i} \right)^{n-1} \tag{20}$$

$$P_e = P(0) = C_n^0 \left(\frac{1}{L_i} \right)^0 \left(1 - \frac{1}{L_i} \right)^n = \left(1 - \frac{1}{L_i} \right)^n \tag{21}$$

$$P_c = 1 - P_s - P_e = 1 - \frac{n}{L_i} \left(1 - \frac{1}{L_i} \right)^{n-1} - \left(1 - \frac{1}{L_i} \right)^n \tag{22}$$

The expected values of successful slots, idle slots, and collision slots in frame F_i, respectively:

$$S_i = L_i * P_s = n \left(1 - \frac{1}{L_i} \right)^{n-1} \tag{23}$$

$$E_i = L_i * P_e = L_i \left(1 - \frac{1}{L_i}\right)^n \tag{24}$$

$$C_i = L_i * P_c = L_i \left\{1 - \frac{n}{L_i}\left(1 - \frac{1}{L_i}\right)^{n-1} - \left(1 - \frac{1}{L_i}\right)^n\right\} \tag{25}$$

As shown in Figure 4, the duration of idle slots, successful slots, and collision slots are, respectively, as follows:

$$t_e = T_{cmd} + T_1 + T_3 \tag{26}$$

$$t_s = T_{cmd} + 2(T_1 + T_2) + T_{RN16} + T_{ACK} + T_{PC+EPC+CRC} \tag{27}$$

$$t_c = T_{cmd} + (T_1 + T_2) + T_{RN16} \tag{28}$$

where T_{cmd} is the time taken by the reader to send the anti-collision commands such as Query/QueryAdjust/QueryRepeat, T_1 is the time measured from the tag antenna port for the reader to transmit to the tag to respond, T_2 is the time for the tag to demodulate the signals sent by the reader, T_3 is the time for the reader to wait before sending the next command after T_1, T_4 is the minimum time interval between commands sent by the reader, T_{RN16} is the time the tag replies to the reader RN16, T_{ACK} is the time the reader sends the ACK command, and $T_{PC+EPC+CRC}$ is the time the tag replies to the reader PC, EPC, and CRC16.

The time efficiency ξ is defined as the statistical average of the ratio of the time occupied by successful slots per frame to the total time within a unit time period, reflecting the system's effective communication capability over a given period:

$$\xi = \frac{1}{k}\sum_{i=1}^{k}\xi_i, 1 \le i \le k \tag{29}$$

where ξ_k represents the time efficiency in frame F_k, and its formula is as follows:

$$\xi_k = \frac{S_k t_s}{T_k} = \frac{S_k t_s}{S_k t_s + C_k t_c + E_k t_e} \tag{30}$$

The identification efficiency η is defined as the total number of tags successfully identified by the reader per unit of time, which directly reflects the system's identification capability:

$$\eta = \sum_{i=1}^{k}S_i, 1 \le i \le k \tag{31}$$

where k denotes the number of frames per unit time and S_k denotes the number of successful slots for the k-th frame.

The throughput th_p is defined as the ratio of the number of successful slots to the total number of slots within a unit of time, reflecting the overall communication efficiency of the system:

$$th_p = \frac{\sum_{i=1}^{k}S_i}{\sum_{i=1}^{k}(E_i + S_i + C_i)}, 1 \le i \le k \tag{32}$$

4.3. Frame Length Estimation

The EPC C1G2 protocol's DFSA anti-collision mechanism stipulates that only the tags selected by the reader through the Select command at the beginning of each frame can participate in the identification process of the current frame [21]. Therefore, in a dynamic environment, for newly arriving tags, the strategy adopted in this paper is that tags arriving

during the current frame do not participate in the identification of that frame. Instead, they will be identified in the next frame. Consequently, the tags to be identified in any frame F_{i+1} are composed of two parts: the tags that were not successfully identified in frame F_i and the newly arrived tags during frame F_i. Thus, the number of tags to be identified in the $(i+1)$-th frame is as follows:

$$r_i = \beta T_i + c_i \tag{33}$$

where β is defined as the tag arrival rate, i.e., the average value of the number of tags newly arriving in the identification area of the reader per unit of time in units of pcs/sec, and when $\beta = 0$, it indicates that the reader is in a static environment with no tags arriving in the tag identification process. T_i is the duration of the frame F_i, and c_i is the number of conflicting tags in the i-th frame. When the tags are uniformly distributed and the system parameters are fixed, the number of tags entering the identification area of the reader in unit time is constant, i.e., the tag arrival rate β is fixed.

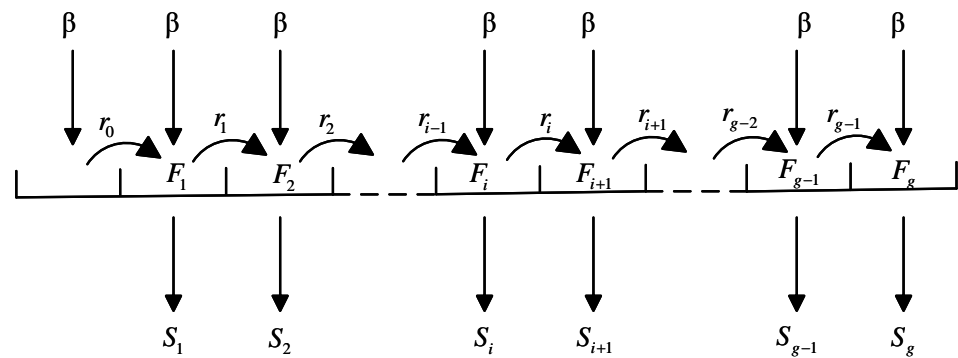The tag identification process is shown in Figure 7.

Figure 7. Tag identification process.

From Section 4.2, we know that the expected values of the successful slots, collision slots, and idle slots in frame F_i are S_i, C_i, and E_i, respectively; hence, we have the following:

$$L_i = S_i + C_i + E_i \tag{34}$$

$$T_i = S_i t_s + C_i t_c + E_i t_e \tag{35}$$

According to Schoute's method [22], it can be known that

$$c_i = 2.39 \times C_i \tag{36}$$

Then,

$$r_i = \beta T_i + c_i = \beta(S_i t_s + C_i t_c + E_i t_e) + 2.39 C_i \tag{37}$$

According to the optimal frame length principle, the maximum channel utilization can be achieved when the frame length is equal to the number of tags to be identified [23]. Therefore, in frame F_{i+1}, the frame length L_{i+1} is as follows:

$$L_{i+1} = r_i = \beta T_i + c_i \tag{38}$$

According to Section 3.1.1, the number of tags entering the reader's identification range per unit of time, i.e., the tag arrival rate β, is as follows:

$$\beta = \begin{cases} \text{round}\left(\dfrac{2\sqrt{d^2 - r^2}}{h}\right) \cdot \dfrac{m_{\text{total}}}{cl} \cdot s, & \dfrac{2\sqrt{d^2-r^2}}{h} < c \text{ and } c \text{ is odd} \\[2ex] \left\lfloor \dfrac{2\sqrt{d^2 - r^2}}{h} \right\rfloor \cdot \dfrac{m_{\text{total}}}{cl} \cdot s, & \dfrac{2\sqrt{d^2-r^2}}{h} < c \text{ and } c \text{ is even} \\[2ex] \dfrac{m_{\text{total}}}{l} \cdot s, & \dfrac{2\sqrt{d^2-r^2}}{h} \geq c \end{cases} \tag{39}$$

4.4. MAC Layer System Status Evaluation Model Based on Combined Weighting-TOPSIS

Using a single method to determine indicator weights can lead to certain biases, resulting in a significant deviation between the calculated results and the actual situation [24]. Therefore, this paper proposes a system status evaluation model for the MAC layer based on the AHP-EW-TOPSIS approach, which combines subjective judgment and objective calculation. The process is shown in Figure 8.
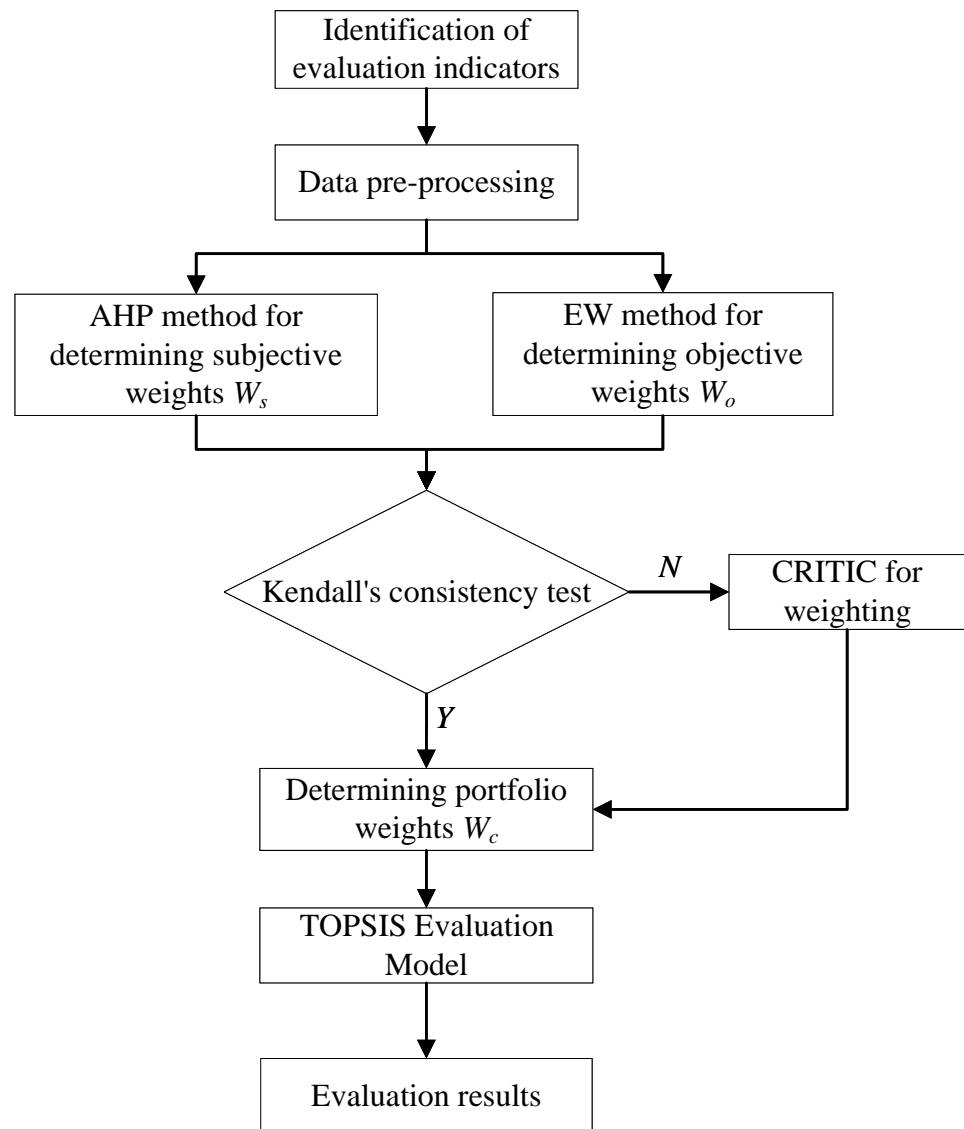

Figure 8. MAC layer system status evaluation model.

4.4.1. Raw Data Processing

(1) Construct a Judgment Matrix

Assume that data from t time points are selected for evaluation, and each time point corresponds to p evaluation criteria, forming a judgment matrix with t rows and p columns.

$$X = \begin{bmatrix} x_{11} & x_{12} & \cdots & x_{1p} \\ x_{21} & x_{22} & \cdots & x_{2p} \\ \vdots & \vdots & \ddots & \vdots \\ x_{t1} & x_{t2} & \cdots & x_{tp} \end{bmatrix} \tag{40}$$

(2) Standardization of Evaluation Metrics

Before evaluating performance indicators, they need to be standardized. Generally, indicators are categorized into three types: positive, negative, and moderate. Different types of indicators are processed using different range-based methods. The evaluation indicators selected in this paper are all positive indicators.

For positive indicators, where larger values are better, the processing method is as follows:

$$y_{ij} = \frac{x_{ij} - x_j^{\min}}{x_j^{\max} - x_j^{\min}} \tag{41}$$

4.4.2. AHP

The Analytic Hierarchy Process (AHP) is a subjective weighting evaluation method that decomposes decision-making problems into more understandable sub-problems and transforms subjective judgments into operable comparisons to achieve quantifiable indicators. Decision-makers can systematically evaluate the interactions between various elements to arrive at a reasonable comprehensive decision. In traditional evaluation algorithms, the AHP is often used to establish a judgment matrix through pairwise comparisons [25]. The judgment matrix $A_{n \times n}$ is defined as follows:

$$A_{n \times n} = \begin{bmatrix} a_{11} & a_{12} & \cdots & a_{1n} \\ a_{21} & a_{22} & \cdots & a_{2n} \\ \vdots & \vdots & \ddots & \vdots \\ a_{n1} & a_{n2} & \cdots & a_{nn} \end{bmatrix} \tag{42}$$

where a_{ij} denotes the level of importance of the i-th evaluation indicator relative to the j-th evaluation indicator. The degree of importance is shown in Table 2.

Table 2. Nine-point scale method and its meaning.

Scale	Meaning
1	Both factors are equally important
3	The former is slightly more important than the latter
5	The former is significantly more important than the latter when comparing the two factors
7	Comparing two factors, the former is more strongly important than the latter
9	The former is extremely more important than the latter when compared to both factors
2, 4, 6, 8	The median of the above neighboring judgments
Reciprocal	If the ratio of the importance of factor i to factor j is a_{ij}, then the ratio of the importance of factor j to factor i is $a_{ji} = \frac{1}{a_{ij}}$

After constructing the judgment matrix $A_{n \times n}$, its eigenvalues and eigenvectors are calculated and the largest eigenvalue $\lambda_{\max}$ as well as the eigenvector $T = [t_1, t_2, \ldots, t_n]$ corresponding to $\lambda_{\max}$ are found.

It is worth noting that when using the AHP to calculate weights, a consistency check of the judgment matrix is required, which is defined as follows:

$$C_R = \frac{C_I}{R_I} \tag{43}$$

where $C_I = \frac{\lambda_{\max} - n}{n-1}$, R_I is the average random consistency index, and its values are shown in Table 3.

Table 3. Random consistency index table.

n	1	2	3	4	5	6	7	8	9
R_I	0	0	0.58	0.90	1.12	1.24	1.32	1.41	1.45

Only when $C_R < 0.1$ is the consistency test passed, at which point the set of weight vectors is $W = \{w_1, w_2, \dots, w_n\}$, where $w_i = \frac{t_i}{\sum_{i=1}^{n} t_i}$.

4.4.3. EW

The entropy weighting (EW) method is an objective evaluation approach [26]. Unlike the AHP, the EW method assigns weights based on the attributes of the data themselves. It evaluates the importance and contribution of each indicator by calculating its entropy value, thereby avoiding the biases introduced by subjective weighting and enhancing the scientific and objective nature of decision-making.

(1) Calculate the entropy e_j

$$e_j = -\frac{1}{\ln m} \sum_{i=1}^{m} \left(Q_{ij} \times \ln Q_{ij} \right) \tag{44}$$

$$Q_{ij} = \frac{x_{ij}}{\sum_{i=1}^{m} x_{ij}} \tag{45}$$

In the above formula, Q_{ij} represents the weight of the i-th evaluated object under the j-th evaluation criterion. To avoid calculation errors caused by zero elements in Q_{ij}, the normalized minimum value can be set to 0.002. If the information entropy e_j of a certain criterion is smaller, it indicates that the fluctuations of the criterion's values are larger, meaning that it provides more information. Therefore, this criterion will have a greater weight in the comprehensive evaluation.

(2) Calculate weight w

$$w = \frac{1 - e_j}{\sum_{j=1}^{n} (1 - e_j)} \tag{46}$$

For the indicator set $X = \{X_1, X_2, \dots, X_p\}$, the corresponding weight set is $W = \{w_1, w_2, \dots, w_p\}$.

4.4.4. AHP-EW Combined Weighting Method

The AHP method and the EW method yield k weight variables $W_1, W_2, \dots, W_k$, with each weight having n observed indicator weight values, meaning that each variable is n-dimensional. Kendall's coefficient of concordance is used to test these weights. If the test passes, it indicates that the weights exhibit concordance; if the test fails, it implies a lack of concordance, suggesting significant differences between the weights.

Let R_{ij} be the rank of W_{ij} in W_j (i.e., the order), and $R_i = \sum_{j=1}^{k} R_{ij}$. The hypothesis testing problem is as follows:

H_0: the K variables are uncorrelated; H_1: the K variables are correlated.

Under the null hypothesis, the ranks in each row do not differ significantly, while under the alternative hypothesis, the ranks differ greatly across the rows. A test statistic can be constructed as follows:

$$T = \sum_{i=1}^{n} \left(R_i - \frac{1}{n} \sum_{i=1}^{n} R_i \right)^2 \tag{47}$$

The Kendall's coefficient of concordance is expressed as follows:

$$W_e = \frac{\sum_{i=1}^{n} \left(R_i - \frac{1}{n} \sum_{i=1}^{n} R_i \right)}{k^2(n^3 - n)} = \frac{\frac{1}{n} \sum_{i=1}^{n} R_i^2 - k^2 n(n+1)/4}{k^2(n^3 - n)/12} \tag{48}$$

One can look up the null distribution table at n fixed

$$k(n-1)W_e > \chi_{n-1}^2 \tag{49}$$

If the test result supports H_1, then H_1 is accepted; otherwise, H_0 is accepted.

If the test is passed, indicating that the weight differences calculated by the AHP method and the EW method are not significant, then the combined weight is as follows:

$$W_c = \frac{W_1 + W_2 + \cdots + W_k}{k} \tag{50}$$

If the test fails, it indicates that there is a significant difference between the weights calculated by the AHP method and the EW method. In this case, the CRITIC method is used to calculate the weights for them, where s_{ij} represents the correlation coefficient between weight i and weight j, and σ_j represents the standard deviation of weight j:

$$C_j = \sigma_j \sum_{i=1}^{m} (1 - s_{ij}) \tag{51}$$

$$\theta_j = \frac{C_j}{\sum_{j=1}^{n} C_j} \tag{52}$$

$$W_c = \theta_1 W_1 + \theta_2 W_2 + \cdots + \theta_k W_k \tag{53}$$

4.4.5. TOPSIS

The Technique for Order Preference by Similarity to Ideal Solution (TOPSIS) is a comprehensive evaluation method that assesses by comparing the proximity of sample data to ideal standard values [27]. This method establishes two extreme reference points in the evaluation space, representing the best and worst states, respectively. The relative closeness of each evaluation object to these reference points is used to characterize its distance. The closer an object is to the optimal point or the farther it is from the worst point, the better its overall characteristics.

The comprehensive weight W_c of the indicators is obtained, and after positive standardization, the data are represented as x'_{ij}. From this, the weighted decision matrix $R = (r_{ij})_{m \times n}$ can be derived, where $r_{ij} = W_c x'_{ij}$.

The maximum value and the minimum value of each indicator (i.e., each column) are defined as r_j^+ and r_j^-, respectively:

$$\begin{cases} r_j^+ = \max(r_{1j}, r_{2j}, \ldots, r_{nj}) \\ r_j^- = \min(r_{1j}, r_{2j}, \ldots, r_{nj}) \end{cases} \tag{54}$$

The distances between the *i*-th evaluation object and the maximum and minimum values are defined as d_j^+ and d_j^-, respectively:

$$\begin{cases} d_i^+ = \sqrt{\sum_{j=1}^n \left(r_j^+ - r_{ij}\right)^2} \\ d_i^- = \sqrt{\sum_{j=1}^n \left(r_j^- - r_{ij}\right)^2} \end{cases} \tag{55}$$

The comprehensive evaluation index of each evaluation object is calculated:

$$Score_i = \frac{d_i^-}{d_i^+ + d_i^-} \tag{56}$$

5. Real-Time Evaluation Model for RFID System Status

5.1. Evaluation Model

Based on the physical layer system status score S_{Phy} and the MAC layer system status score S_{MAC}, this paper classifies the RFID system status into four categories and proposes an RFID system status evaluation model based on CART. The classification method is shown in Figure 9, where the Level I system status is the best, and the Level IV system status is the worst.
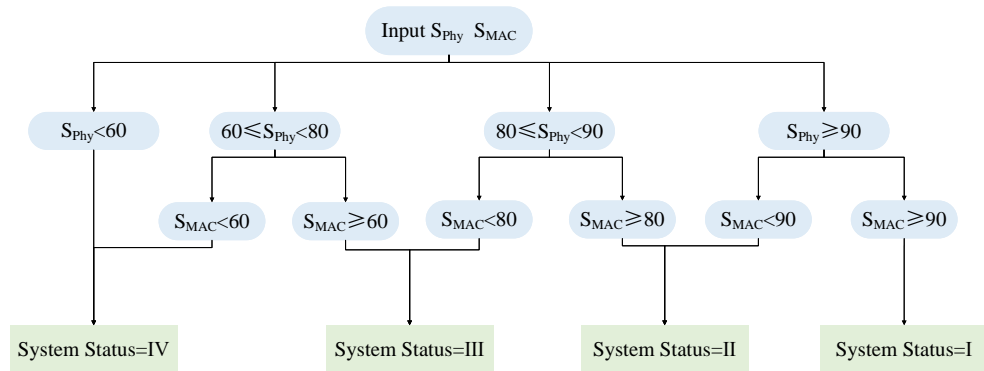
Figure 9. RFID system status classification.

5.2. RFID System Status Evaluation Model Based on CART

Decision tree is a supervised learning technique and a classification algorithm based on a tree structure that classifies data through a series of rules [28]. The CART (Classification and Regression Tree) algorithm used in this paper is one of the classic algorithms of decision trees. Compared to other decision tree algorithms, CART splits the data recursively using a binary tree. The core idea of CART is to select the optimal split point at each step, dividing the dataset into two subsets to maximize the purity of the subsets. The decision tree generated by CART has high interpretability, can effectively capture nonlinear relationships in the data, and is fast to train, making it particularly suitable for large-scale datasets. The algorithm flow is as follows:

Step 1: Selecting the Best Split Point. The CART decision tree uses the Gini index as the measure for splitting nodes and selects the feature with the smallest Gini index as the best splitting feature.

For a specific value *a* of a feature *A*, after splitting the dataset *D* into two subsets D_1 and D_2, the formula for calculating the Gini index is as follows:

$$gini\_index = \frac{|D_1|}{|D|} gini(D_1) + \frac{|D_2|}{|D|} gini(D_2) \tag{57}$$

$$gini(a_i) = 1 - \sum_i (p_i^2) \tag{58}$$

where p_i denotes the proportion of the number of samples in a category to the total number of samples. The smaller the *gini*, the more evenly distributed the samples.

Step 2: Recursively Build the Decision Tree. Apply the splitting method at each node recursively until a stopping criterion is met (for example, the number of samples in a node is below a threshold or the Gini index is below a threshold).

Step 3: Pruning. After building the complete tree, pruning is used to remove parts of the tree that may lead to overfitting. CART typically uses cost-complexity pruning, which minimizes a cost-complexity function.

Step 4: Classification and Prediction. For a new sample, the CART algorithm starts from the root of the tree and moves down through the splits based on the sample's feature values until reaching a leaf node. The class of the leaf node is the predicted result for that sample.

6. Calculation and Analysis of Real-Time Status Evaluation

6.1. Test Scenario

The test scenario is set up in a spacious indoor environment. The archive shelf has five levels, with a length of 2.5 m, a height of 2 m, and a shelf height of 0.4 m. A total of 100 archive boxes, each randomly placed on the shelf, are affixed with 900 MHz UHF passive RFID tags on their sides. The choice of these tags and the reader is based on their common use and performance in industrial applications. A mobile robot (Water robot) equipped with an Impinj SpeedWay Reader and a 9 dBi circularly polarized antenna moves parallel to the archive shelf at different speeds to perform tag identification tests.

The spectrum analyzer (Keysight N9010B) used in the tests is employed to capture the interaction process between the reader and the tag in order to analyze time slot information. All the test data are collected under the same environmental conditions to ensure data consistency and comparability.

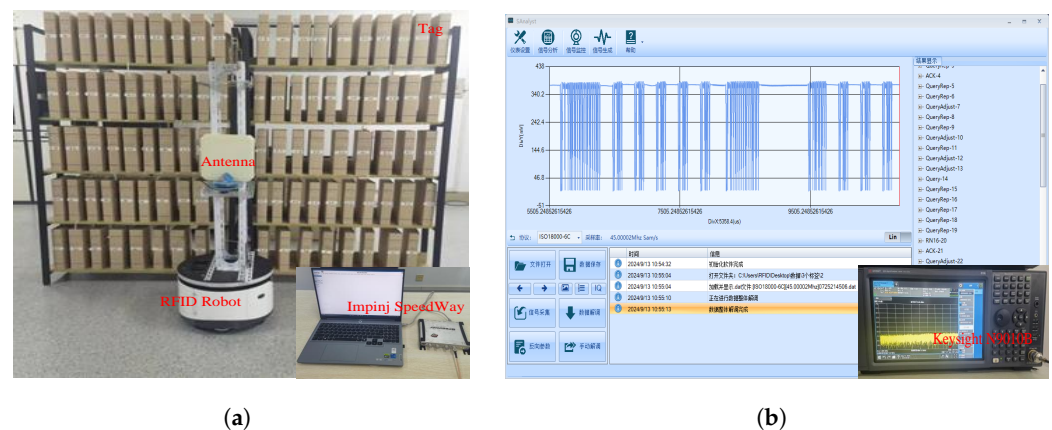The test scenario is illustrated in Figure 10, and the test equipment is detailed in Table 4.

(**a**)   (**b**)

Figure 10. Test scenario. (**a**) Archive shelf test scenario. (**b**) Spectrum analyzer test scenario.

In the process of mobile identification, an orthogonal table based on the number and levels of the RFID system parameters from Table 5 is designed. Then, the RFID system parameters according to the combination forms in the orthogonal table are tested. For each parameter combination, 50 tests are conducted, and the average is taken. A comprehensive analysis of the impact of different parameter combinations on the system's performance is conducted.

Table 4. System equipment selection and performance specifications.

Equipment	Equipment Parameters
RFID Tags	UHF 900 MHz electronic tag
Reader	Impinj SpeedWay Reader
Antenna	9 dBi circular polarization reader antenna
RFID Robot	Water robot
Spectrum Analyzer	Keysight N9010B

Table 5. RFID system parameters.

Parameters	Parameter Value	Parameter Unit
Reader–Tag Distance	0.5, 1, 1.5, 2	m
Reader Power	20–30	dBm
Reader Frequency	920.625	MHz
Robot Speed	0.1–0.7	m/s

6.2. Verification of the RFID System Status Evaluation Model

6.2.1. Verification of the MAC Layer System Status Evaluation Model

(1) Indicator Preprocessing

The performance indicators selected in this paper are the throughput per unit time X_1, identification efficiency X_2, and time efficiency X_3, which are obtained by analyzing the time slot information collected by a spectrum analyzer during the movement of the RFID robot. All three are positive indicators, and the positive indicator processing method is used.

(2) Determination of Index Weights

Using subjective weights to assign scores to the importance of different performance indicators, the judgment matrix is constructed as follows:

$$H_1 = \begin{bmatrix} 1 & 3 & 5 \\ \frac{1}{3} & 1 & 2 \\ \frac{1}{5} & \frac{1}{2} & 1 \end{bmatrix}, \quad H_2 = \begin{bmatrix} 1 & 2 & 3 \\ \frac{1}{2} & 1 & 2 \\ \frac{1}{3} & \frac{1}{2} & 1 \end{bmatrix}, \quad H_3 = \begin{bmatrix} 1 & 1 & 3 \\ 1 & 1 & 3 \\ \frac{1}{3} & \frac{1}{3} & 1 \end{bmatrix} \tag{59}$$

An approximate solution method is used to calculate the eigenvector of the judgment matrix, and a consistency check is performed to obtain the subjective weights:

$$W_s = (W_1, W_2, \ldots, W_3) \tag{60}$$

$$\begin{cases} W_1 = (0.6483, 0.2297, 0.1220) \\ W_2 = (0.5396, 0.2970, 0.1634) \\ W_3 = (0.4286, 0.4286, 0.1429) \end{cases} \tag{61}$$

The indicator data of each set of parameters are input into the EW method to calculate the objective weights W_o of each indicator:

$$W_o = (0.4427, 0.4455, 0.1118) \tag{62}$$

The comprehensive weight W_c is as follows:

$$W_c = (0.4908, 0.3819, 0.1273) \tag{63}$$

Based on Equation (63), throughput is the most critical metric for evaluating the system status of the MAC layer in RFID systems.

(3) Combined Weighting-TOPSIS Comprehensive Evaluation

Based on the weighted decision matrix $R = (r_{ij}^{m \times n})$, using Equation (54), the best solution matrix $f^*(+)$ and the worst solution matrix $f^*(-)$ for the model are obtained, respectively, as follows:

$$\begin{cases} f^*(+) = (0.0011, 0.0008, 0.0003) \\ f^*(-) = (0.8688 \times 10^{-3}, 0.6769 \times 10^{-3}, 0.2389 \times 10^{-3}) \end{cases} \quad (64)$$

Figure 11 illustrates the comparison between the real-time throughput and MAC layer system status during the 60 s movement of the RFID robot. It can be observed that the throughput fluctuations of the RFID robot remain relatively stable during movement, making it difficult to intuitively reflect the instantaneous changes in the system status. In contrast, the multi-indicator integrated system status sensing model can provide a finer granularity, clearly revealing the dynamic changes in the MAC layer system status. This indicates that the multi-indicator system status sensing model is more aligned with the actual evaluation and decision-making process, offering more accurate evaluation results.
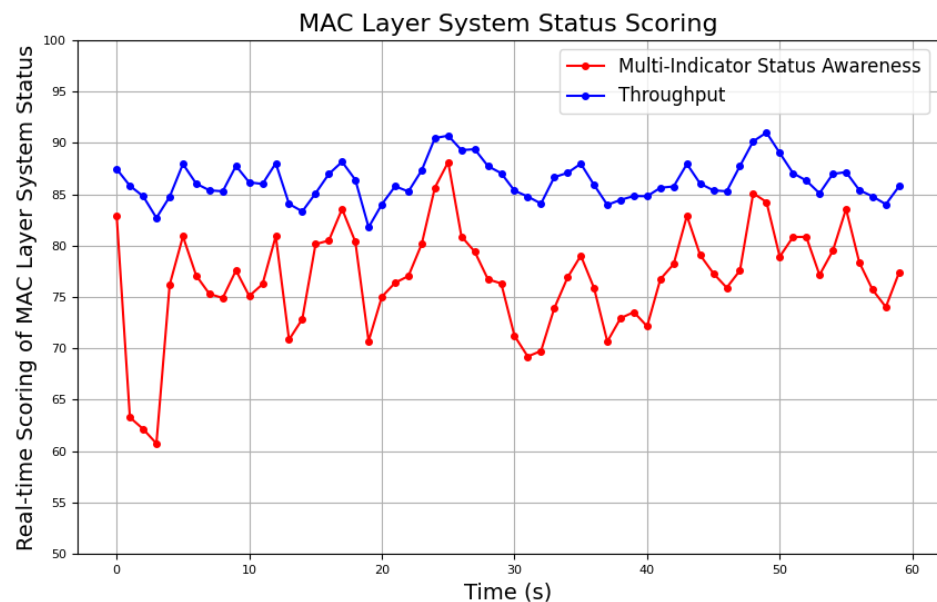
Figure 11. MAC layer system status scoring.

6.2.2. Validation of the Physical Layer Link Quality Evaluation Model

The dataset used for evaluating the physical layer link quality consists of nonlinear, high-dimensional data. To improve the efficiency of the data analysis and the accuracy of its structure, this paper adopts the nonlinear dimensionality reduction algorithm UMAP to perform dimensionality reduction, extracting three link feature parameters. Furthermore, the K-Means algorithm is used to cluster these link feature parameters, and the entropy weight method is applied to calculate the weights of various indicators. The clusters are then weighted and ranked, dividing the link quality into five levels, ranging from Level I (best) to Level V (worst). The weightings of the various indicators are shown in Table 6, while the weight distribution of variance, kurtosis, and skewness in the signal strength under the LQVI is shown in Table 7. The clustering results are depicted in Figure 12. The average silhouette coefficient is 0.70184, indicating high cohesion and separation, with clear cluster boundaries and good clustering performance.

According to the K-Means algorithm, the value range of the link parameters at different link levels is shown in Table 8.

Table 6. Indicator weighting.

Indicator	Weighting
$\overline{RSSI}$	0.2746
LQVI	0.1353
BER	0.1996
RoI	0.1902
Number of Inventory	0.2003

Table 7. Weightings of each indicator in LQVI.

Indicator	Weighting
σ^2_{RSSI}	0.3161
Skewness	0.3048
Kurtosis	0.3791
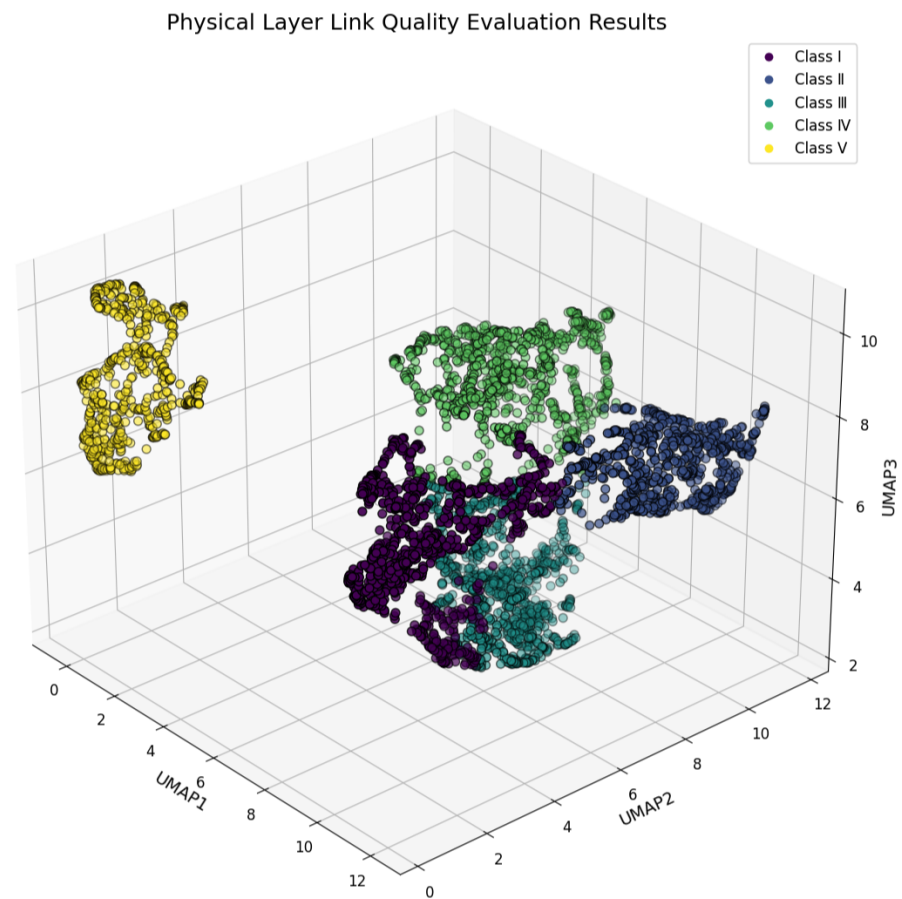
Figure 12. Link quality evaluation results.

Table 8. Link levels and parameter ranges.

Link Level	$\overline{RSSI}$	LQVI	Number of Inventory	BER	RoI
Class I	−56.36∼46.54	0.009∼0.312	77∼176	0.001∼0.046	0.226∼0.985
Class II	−65.23∼48.97	0.069∼0.286	12∼152	0.001∼0.031	0.381∼0.973
Class III	−65.74∼51.30	0.015∼0.164	17∼128	0.001∼0.037	0.500∼0.988
Class IV	−66.15∼50.55	0.114∼0.361	15∼80	0.001∼0.043	0.108∼0.988
Class V	−66.02∼48.48	0.016∼0.287	12∼58	0.001∼0.047	0.111∼0.985

6.2.3. Verification of the RFID System Status Evaluation Model

The system status scores of the physical layer and MAC layer are integrated into a new dataset as input for the CART algorithm to classify the RFID system status. The input data are split into a training set and a test set in a 7:3 ratio, and the CART algorithm is used for evaluation. The results are shown in Table 9. The sample distribution is shown in Figure 13, where red markings indicate misclassified samples.

Table 9. Evaluation of classification algorithms.

System Status Class	Accuracy ACU	Recall	F1-Score
Class I	100.0%	0.930	0.964
Class II	95.8%	0.986	0.971
Class III	98.3%	0.991	0.987
Class IV	99.1%	0.991	0.991
Total	98.3%	-	-
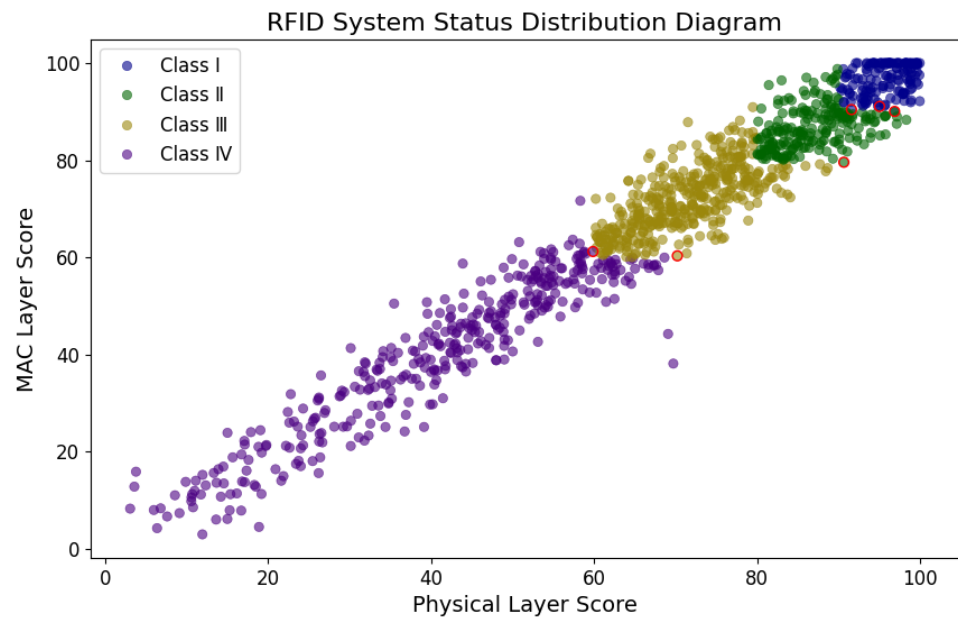
Figure 13. Classification results of RFID system status, where red markings indicate misclassified samples.

To evaluate the performance of the CART-based RFID system status evaluation method with different numbers of tags, test scenarios were set up with 50 and 150 tags, respectively, and RFID system status evaluations were conducted. The CART classification results are shown in Table 10.

Table 10. Classification accuracy under different numbers of tags.

Tag Density	Accuracy
Low	98.7%
Medium	98.3%
High	92.1%

This paper selects the Support Vector Machine (SVM), Random Forest (RF), Gaussian Naive Bayes (GNB), and Multilayer Perceptron (MLP) algorithms to compare with the status evaluation method of an RFID system based on CART. Classification accuracy and algorithm running time are used as performance evaluation criteria. The same dataset is

used to train the aforementioned algorithm models, and 1000 test set samples are used for classification. The performance comparison of different algorithms is shown in Figure 14, and the classification accuracy and running time are presented in Table 11. The results show that the RFID system status evaluation method based on CART has a shorter running time and higher classification accuracy.
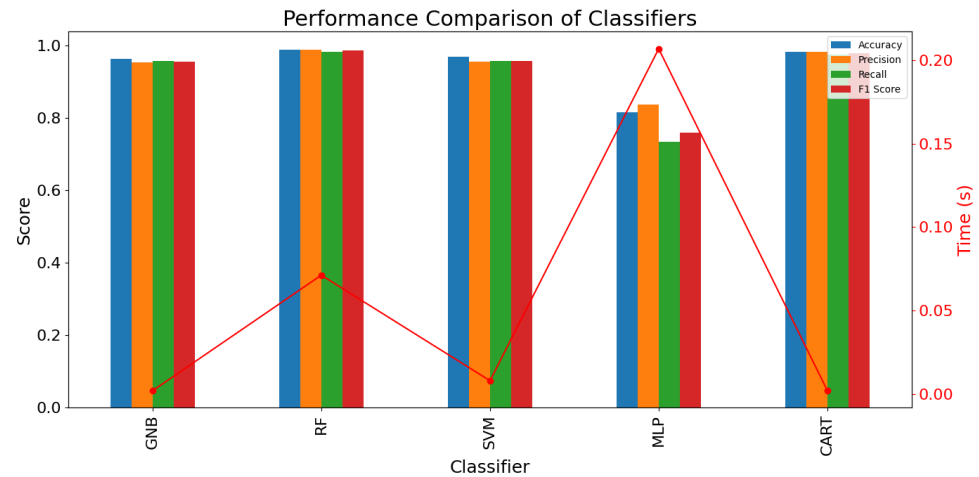

Figure 14. Comparison of classification algorithm performance.

Table 11. Comparison of different algorithms.

Algorithm	Running Time (s)	Test Set Accuracy
GNB	0.003	96.2%
RF	0.147	98.8%
SVM	0.015	96.8%
MLP	0.364	81.6%
CART	0.003	98.3%

6.3. Practical Applications and Engineering Contributions

This paper proposes a system for the real-time status evaluation of UHF passive RFID robots in dynamic scenarios, providing an effective tool for evaluating and optimizing the performance of RFID systems in such environments. By monitoring and analyzing the RFID system's behavior in real time within dynamic settings, engineers can promptly adjust system parameters and optimize resource allocation, thereby enhancing the system's robustness and adaptability. This method not only reduces misreads and missed reads, improving recognition accuracy, but also supports intelligent decision-making by automatically adjusting the system to accommodate environmental changes, such as reader movement or changes in the number of tags. Moreover, this study promotes the integration of RFID technology with emerging technologies, offering technical support for the development of new application scenarios and the enhancement of performance in existing applications. This helps reduce operational costs, improve user experience, and drive the establishment of relevant industry standards. In summary, this research lays a solid theoretical and practical foundation for the widespread application of RFID technology in various fields, such as logistics, retail, and smart manufacturing, injecting new momentum into the digital transformation and intelligent upgrading of industries.

7. Conclusions

This paper first elaborates on the theoretical foundation of the real-time evaluation of the RFID system status in dynamic scenarios and highlights its critical role in improving the efficiency of RFID robot systems. It proposes different perspectives for evaluating the status of the RFID system. Then, it presents a real-time evaluation method for the MAC layer

status of UHF passive RFID robot systems in dynamic scenarios, based on a combination weighting-TOPSIS approach. Additionally, it introduces a real-time evaluation method for physical layer link quality based on UMAP and K-Means, and by integrating the results of both evaluations, it proposes a real-time RFID system status evaluation method using CART. Finally, through comparison with other algorithms, the results demonstrate that the method proposed in this paper achieves an accuracy of 98.3% and an algorithm runtime of 0.003 s, outperforming other algorithms. This method is highly suitable for the real-time evaluation of the RFID robot system status in dynamic scenarios.

Considering the requirements for RFID system status evaluation in dynamic scenarios, future research will focus on the following two aspects:

1. The generalization ability of existing models is limited, especially when applied to more complex or diverse dynamic scenarios, where the model's performance may degrade. Future research will emphasize training with more diverse scenarios, using a broader range of scene data to train models. This will enhance their generalization ability, ensuring stability in complex environments.

2. The focus will be on designing adaptive recognition algorithms and adjustment strategies based on system status evaluation results. This will optimize the RFID system status in dynamic scenarios, ultimately achieving intelligent awareness of the system status in these environments.

References

1. Kokkonen, M.; Myllymäki, S.; Putaala, J.; Jantunen, H. A Resonator Enhanced UHF RFID Antenna Cable for Inventory and Warehouse Applications. *IEEE J. Radio Freq. Identif.* **2022**, *6*, 128–133. [CrossRef]
2. Škiljo, M.; Šolić, P.; Blažević, Z.; Rodić, L. D.; Perković, T. UHF RFID: Retail Store Performance. *IEEE J. Radio Freq. Identif.* **2022**, *6*, 481–489. [CrossRef]
3. Khan, Z.; Chen, X.; He, H.; Xu, J.; Wang, T.; Cheng, L.; Ukkonen, L.; Virkki, J. Glove-Integrated Passive UHF RFID Tags: Fabrication, Testing and Applications. *IEEE J. Radio Freq. Identif.* **2019**, *3*, 127–132. [CrossRef]
4. Zhao, N.; Zhang, L.; Lei, L.; Cai, S. Dynamic Query Tree Anti-Collision Protocol for RFID Systems. In Proceedings of the 2019 IEEE 25th International Conference on Parallel and Distributed Systems (ICPADS), Tianjin, China, 4–6 December 2019. [CrossRef]
5. Montanaro, T.; Sergi, I.; Motroni, A.; Buffi, A.; Nepa, P.; Pirozzi, M.; Catarinucci, L.; Colella, R.; Chietera, F.P.; Patrono, L. An IoT-Aware Smart System Exploiting the Electromagnetic Behavior of UHF-RFID Tags to Improve Worker Safety in Outdoor Environments. *Electronics* **2022**, *11*, 717. [CrossRef]
6. Ehrenberg, I.; Floerkemeier, C.; Sarma, S. Inventory Management with an RFID-equipped Mobile Robot. In Proceedings of the 2007 IEEE International Conference on Automation Science and Engineering, Scottsdale, AZ, USA, 22–25 September 2007; pp. 1020–1026. [CrossRef]
7. Bernardini, F.; Motroni, A.; Nepa, P.; Tripicchio, P.; Buffi, A.; Del Col, L. The MONITOR Project: RFID-based Robots enabling real-time inventory and localization in warehouses and retail areas. In Proceedings of the 2021 6th International Conference on Smart and Sustainable Technologies (SpliTech), Bol and Split, Croatia, 8–11 September 2021; pp. 1–6. [CrossRef]
8. Mylonopoulos, G.; Chatzistefanou, A.R.; Filotheou, A.; Tzitzis, A.; Siachalou, S.; Dimitriou, A.G. Localization, Tracking and Following a Moving Target by an RFID Equipped Robot. In Proceedings of the 2021 IEEE International Conference on RFID Technology and Applications (RFID-TA), Delhi, India, 6–8 October 2021; pp. 32–35. [CrossRef]

9.   Cecchi, G.; Motroni, A.; Ria, A.; Nepa, P. Obstacle-Avoidance through RFID Near-Field Detectors for Robot-Based Localization and Sensing Systems. In Proceedings of the 2024 9th International Conference on Smart and Sustainable Technologies (SpliTech), Bol and Split, Croatia, 25–28 June 2024; pp. 1–5. [CrossRef]

10.   Madanian, S.; Parry, D. Identifying the Potential of RFID in Disaster Healthcare: An International Delphi Study. *Electronics* **2021**, *10*, 2621. [CrossRef]

11.   Sharif, A.; Yan, Y.; Ouyang, J.; Chattha, H.T.; Arshad, K.; Assaleh, K.; Alotabi, A.A.; Althobaiti, T.; Ramzan, N.; Abbasi, Q.H.; et al. Uniform Magnetic Field Characteristics Based UHF RFID Tag for Internet of Things Applications. *Electronics* **2021**, *10*, 1603. [CrossRef]

12.   Ramakrishnan, K.M.; Deavours, D.D. Performance Benchmarks for Passive UHF RFID Tags. In Proceedings of the 13th GI/ITG Conference—Measuring, Modelling and Evaluation of Computer and Communication Systems, Nurnberg, Germany, 27–29 March 2006; pp. 1–18.

13.   ODIN. *The Gen 2 RFID Reader Benchmark: The Winners Circle*; ODIN: Dulles, VA, USA, 2006.

14.   Aroor, S.R.; Deavours, D.D. Evaluation of the State of Passive UHF RFID: An Experimental Approach. *IEEE Syst. J.* **2007**, *1*, 168–176. [CrossRef]

15.   Periyasamy, M.; Dhanasekaran, R. Evaluation of Performance of UHF Passive RFID System in Metal and Liquid Environment. In Proceedings of the 2015 International Conference on Communications and Signal Processing (ICCSP), Melmaruvathur, India, 2–4 April 2015; pp. 0414–0417. [CrossRef]

16.   Li, T.; Wang, D. Experimental Studying Measurement Metrics of RFID System Performance. In Proceedings of the 2009 3rd International Conference on Anti-Counterfeiting, Security, and Identification in Communication, Hong Kong, China, 20–22 August 2009; pp. 233–237. [CrossRef]

17.   Xie, L.; Li, Q.; Wang, C.; Chen, X.; Lu, S. Exploring the Gap between Ideal and Reality: An Experimental Study on Continuous Scanning with Mobile Reader in RFID Systems. *IEEE Trans. Mob. Comput.* **2015**, *14*, 2272–2285. [CrossRef]

18.   Myasnikov, E. Using UMAP for Dimensionality Reduction of Hyperspectral Data. In Proceedings of the 2020 International Multi-Conference on Industrial Engineering and Modern Technologies (FarEastCon), Vladivostok, Russia, 6–9 October 2020; pp. 1–5. [CrossRef]

19.   Wahyuningrum, T.; Khomsah, S.; Suyanto, S.; Meliana, S.; Yunanto, P.E.; Al Maki, W.F. Improving Clustering Method Performance Using K-Means, Mini Batch K-Means, BIRCH and Spectral. In Proceedings of the 2021 4th International Seminar on Research of Information Technology and Intelligent Systems (ISRITI), Yogyakarta, Indonesia, 16–17 December 2021; pp. 206–210. [CrossRef]

20.   Guo, J.; Lin, J.; Zhang, Z.; Ling, H. CDBSCAN: Density clustering based on silhouette coefficient constraints. In Proceedings of the 2022 International Conference on Computer Engineering and Artificial Intelligence (ICCEAI), Shijiazhuang, China, 22–24 July 2022; pp. 600–605. [CrossRef]

21.   *ISO/IEC 18000-6*; Information Technology—Radio Frequency Identification for Item Management—Part 6: Parameters for Air Interface Communications at 860 MHz to 960 MHz. ISO: Geneva, Switzerland, 2006.

22.   Schoute, F. Dynamic Frame Length ALOHA. *IEEE Trans. Commun.* **1983**, *31*, 565–568. [CrossRef]

23.   Chen, W.-T. Optimal Frame Length Analysis and an Efficient Anti-Collision Algorithm with Early Adjustment of Frame Length for RFID Systems. *IEEE Trans. Veh. Technol.* **2016**, *65*, 3342–3348. [CrossRef]

24.   Mou, Y.-P.; Zhang, Y.; Gao, X.-R.; Peng, J.-P.; Qiu, C.-R.; Liu, D.-Z. Evaluation of Wheelset Re-profiling Strategies Based on Combination Weighting TOPSIS. In Proceedings of the 2021 IEEE Far East NDT New Technology & Application Forum (FENDT), Kunming, China, 14–17 December 2021; pp. 39–43. [CrossRef]

25.   Dong, Y.; Hong, W.-C.; Xu, Y.; Yu, S. Selecting the Individual Numerical Scale and Prioritization Method in the Analytic Hierarchy Process: A 2-Tuple Fuzzy Linguistic Approach. *IEEE Trans. Fuzzy Syst.* **2011**, *19*, 13–25, [CrossRef]

26.   Zhang, X.; Li, W.; Cui, W. Study on Health Status of Higher Education Based on Entropy Weight-Topsis and Logistic Model. In Proceedings of the 2021 2nd International Conference on Big Data and Informatization Education (ICBDIE), Hangzhou, China, 2–4 April 2021; pp. 415–418. [CrossRef]

27.   Dutta, B.; Dao, S.D.; Martínez, L.; Goh, M. An evolutionary strategic weight manipulation approach for multi-attribute decision making: TOPSIS method. *Int. J. Approx. Reason.* **2021**, *129*, 1–25. [CrossRef]

28.   Rahmatillah, I.; Astuty, E.; Sudirman, I.D. An Improved Decision Tree Model for Forecasting Consumer Decision in a Medium Groceries Store. In Proceedings of the 2023 IEEE 17th International Conference on Industrial and Information Systems (ICIIS), Peradeniya, Sri Lanka, 25–26 August 2023; pp. 245–250. [CrossRef]